ELSEVIER

Journal of Pharmaceutical and Biomedical Analysis
30 (2002) 197–208

JOURNAL OF
PHARMACEUTICAL
AND BIOMEDICAL
ANALYSIS

www.elsevier.com/locate/jpba

Formation of novel toxic compounds from oxidative interaction between salsolinol and cysteine

Fa Zhang *

Johnson & Johnson C&PC RD&E, Skillman, NJ 08558, USA

Received 9 July 2001; accepted 3 April 2002

Abstract

The electrochemically-driven oxidation of salsolinol (SAL) precedes via a 2e, $2H^+$ process to produce the corresponding *o*-quinone (E) intermediate which has a very short lifetime and can be scavenged by cysteine to give the corresponding adduct cysteinyl salsoninol (F). F is more easily oxidized to the corresponding *o*-quinone (G) followed by cyclization resulting in the formation of the quinone imine intermediate (H). H can then undergo series of nucleophilic addition and oxidation reactions to produce a very complicated mixture of products including some dihydrobenzothiazines. Six of these products have been isolated and identified. Central administration of these compounds into laboratory mice revealed that three of them are fairly toxic and evoke profound behavioral responses.

Keywords: Salsolinol; Cysteine; Oxidation; HPLC; Cyclic voltammetry

1. Introduction

Catecholamine derivatives are widely found in nature and serve in diverse biological processes such as in melanization of human skin, hair, eye, central nervous system (CNS) [1–5]. Central to the metabolism of catecholamines is their oxidation to form the corresponding quinone intermediates, which could yield polymeric eumelanin products or react with external nucleophiles to account for pheomelanin products. Concomitantly, generation of toxic intermediates or products including active oxygen radicals could occur, which might disorder the normal biological processes, or enhance the processes which we really want to slow down, such as aging. Salsolinol (SAL) is a trace constituent of the mammalian biological system and a Pictet–Spengler condensation product of the neurotransmitter dopamine with acetaldehyde, the proximate metabolite of ethanol [6].

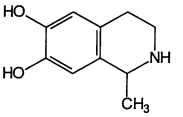

Salsolinol (SAL)

The level of SAL in certain brain regions of rats is elevated when they chronically consume ethanol [7]. In humans, the urinary level of SAL is elevated

* Tel.: +1-908-874-1333; fax: +1-908-874-1252
E-mail address: fzhang1@cpcus.jnj.com (F. Zhang).

0731-7085/02/$ - see front matter © 2002 Published by Elsevier Science B.V.
PII: S0731-7085(02)00383-7

during ethanol intoxication and declines with detoxification [8]. SAL and other tetrahydroisoquinolines (TIQs) have been speculated to contribute to the behavior changes, addictive properties and neurodamage in brains of alcoholics [9]. It has also been proposed that the oxidation of SAL and other TIQs, which are elevated in the brain of intoxicated individuals, might lead to the formation of toxins which are responsible for the neurodamage. We have previously [10,11] demonstrated (Scheme 1) that the initial oxidation of SAL was a reversible 2e, $2H^+$ reaction giving an *o*-quinone (E) which had a very short lifetime at physiological pH and was involved in tautomerizations and/or nucleophilic addition reactions to generate A, B, C and D. E is also quite susceptible to reaction with cysteine (CySH), one of the intraneuronal nucleophiles and a well-known antioxidant, to form 8-*S*-cysteinylsalsolinol (F) which is more easily oxidizable than the parent SAL. F can be oxidized to the corresponding *o*-quinone G which can cyclize to give the quinone imine H. H can then produce dihydrobenzothiazine (I) as a final product. Hence it can be expected that in the oxidation of SAL, the endogenous nucleophiles such as cysteine, glutathione or cysteinyl residues of protein could participate in to scanvage the proximate quinone E yielding the corresponding adducts or benzothiazine species similar to that described in Scheme 1. In addition, our previous results [10,11] (Scheme 1) also indicated that the cysteinyl adducts or dihydrobenzothiazine species from SAL are more easily oxidizable than the parent SAL. Accordingly further oxidation of these compounds could yield more complicated products. The purpose of

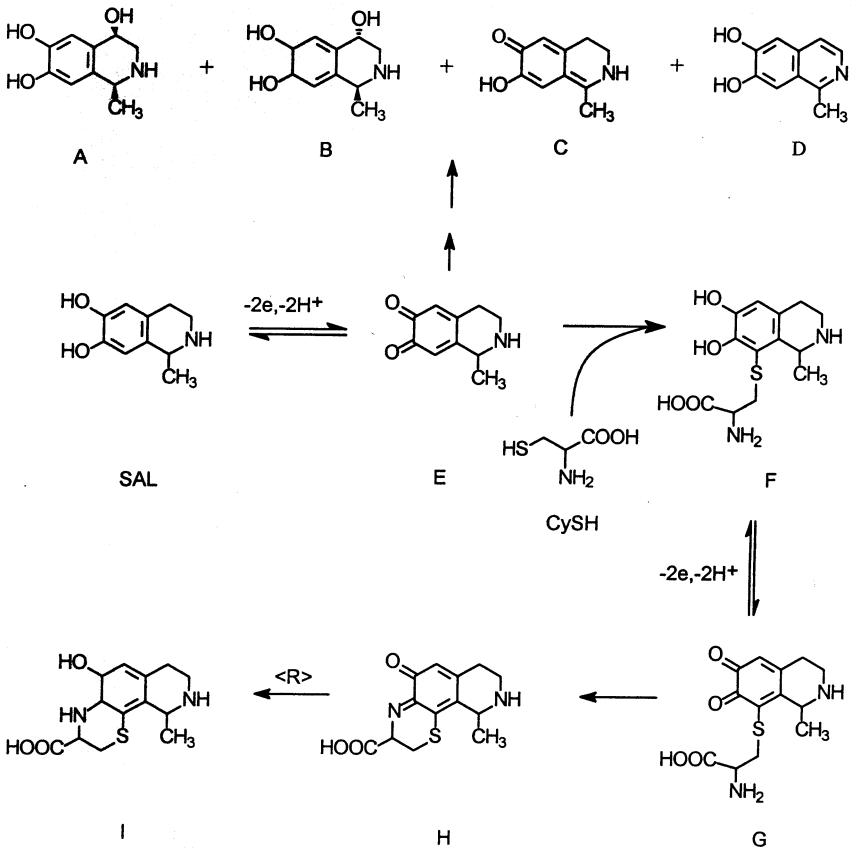

Scheme 1.

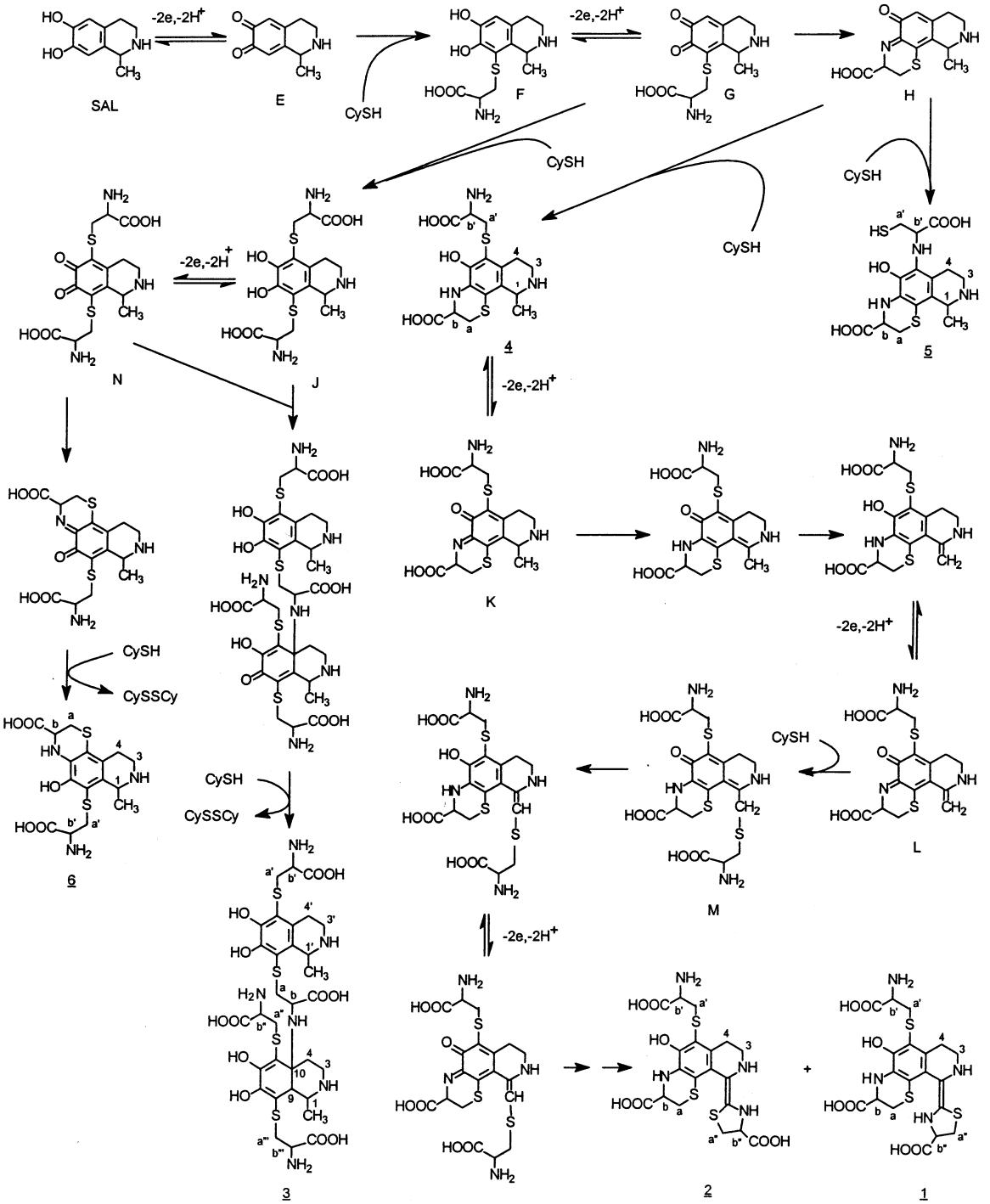

Scheme 2.

this report is to provide further insights into the effects of L-cysteine on the oxidation chemistry of SAL. The electrochemical oxidation of SAL in the presence of L-cysteine was investigated. Six new novel products were isolated and structurally identified. A more detailed reaction mechanism was proposed (Scheme 2). Preliminary biological tests revealed that some of the products are potent neurotoxins. These results may provide valuable insight into the fundamental oxidation chemistry of SAL in vivo and could be helpful for the understanding of the pathoetiology of related biological disorders.

2. Experimental

2.1. Chemicals

L-SAL hydrochloride and L-cysteine were obtained from Sigma (St. Louis, MO) and were used without additional purification. Phosphate buffers of known ionic strength were prepared according to Christian and Purdy [12].

2.2. Apparatus

Voltammograms were obtained at a pyrolytic electrode (PGE, Pfizer Minerals, Pigments and Metals Division, Easton, PA) having an approximate surface area of 4 mm^2. A conventional three-electrode voltammetric cell containing a platinum wire counter electrode and a saturated calomel reference electrode (SCE) were used in addition to the pyrolytic electrode. Cyclic voltammograms were obtained with a BAS-100A (Bioanalytical System, West Lafeyette, IN) instrument. Voltammograms were corrected for iR drop and the PGE was resurfaced before recording each voltammogram using standard procedures [13]. Controlled potential electrolysis employed a Princeton Applied Research Corporation (Princeton, NJ) Model 173 potentiostat. The working electrode consists of several plates of pyrolytic graphite having a total surface area of approximately 430 cm^2. In the three-electrode cell the working, counter and reference electrode compartments were separated with a Nafion membrane (type 117, Dupont Co., Wilmington, DE). The working electrode compartment had a capacity of 80 ml. The counter electrode was platinum wire that was suspended into the appropriate supporting electrolyte. The solution in the working electrode compartment was bubbled vigorously with N_2 gas. All potentials are referred to the SCE at ambient temperature (22 ± 2 °C).

^{1}H NMR spectra were recorded using a Varian XL-300 spectrometer. Low and high-resolution fast atom bombardment mass spectrometry (FAB-MS) was carried out with a VG (Manchester, UK) Model ZAB-E spectrometer. Ultraviolet–visible spectra were recorded on a HP 8452A diode array spectrophotometer.

High performance liquid chromatography (HPLC) employed a Gilson (Middleton, WI) binary gradient system equipped with 305 and 306 pumps and a Holochrome UV detector set at 254 nm. Two preparative reversed phase columns were employed throughout this study: a Spherisorb column (S10, ODS2, 25×2 cm, Phase Sep., Clwyd, UK) and a Regis column (ODS, 25×2.1 cm, Morton Grove, IN). A short guard column (Upchurch, C1022, 1×1 cm) packed with Bakerbond (J.T. Baker, C18, 10 μm particle size) was employed. Four mobile phase solvents were used. Solvent A was prepared by adding 30 ml of concentrated ammonium hydroxide solution to 4 l of deionized water; the pH of this solution was then adjusted to 3.0 by addition of trifluoroacetic acid (TFA). Solvent B was prepared by adding 30 ml of concentrated ammonium hydroxide solution to 1 l of HPLC grade methanol and 1 l of HPLC grade acetonitrile and 2 l of deionized water. The pH of this solution was adjusted to 3.0 by addition of TFA. Solvent C was prepared by adding TFA to deionized water until the pH became 3.0. Solvent D was prepared by adding TFA to 1:1 (v/v) solution of acetonitrile and water and the pH was adjusted to 3.0. For HPLC Method I, the following gradient was employed. Zero to two minutes, 100% solvent A, 2–10 min, linear gradient to 20% solvent B, 10–60 min, linear gradient to 60% solvent B, 60–80 min, linear gradient to 100% solvent B, 80–90 min, 100% Solvent B. The flow rate was 7 ml/min. For HPLC Method II, the following gradient was used: 0–2 min, 100%

solvent C, 2–20 min, linear gradient to 20% solvent D, 20–25 min, linear gradient to 100% solvent D, 25–30 min, 100% D. The flow rate was 7 ml/min. For HPLC Method III, the following gradient was used: 0–2 min, 100% solvent C, 2–20 min, linear gradient to 40% solvent D, 20–25 min, linear gradient to 100% solvent D, 25–35 min, 100% solvent D. The flow rate was 7 ml/min.

In vivo experiments employed outbred adult male mice of the Hsd:ICR albino strain (Harlan Sprague–Dawley, Madison, WI) weighing 35 ± 4 g. The animals were housed ten per cage, allowed access to Purina Rat Chow and water ad libitum, and maintained on a 12-h light:12-h dark cycle with lights on at 07:00 h. Mice were not used in experiments until at least 7 days after receipt from the supplier. Experimental animals were treated with test drugs dissolved in isotonic saline (0.9% NaCl in deionized water). Animals were first anesthetized with ether for 30–45 s. Injection of maximum volume of 5 μl solution was performed free hand. The site of puncture is approximately 3.5 mm anterior to the interaural line and 1 mm right lateral of the middle line perpendicular to the scalp to a depth of 3 mm. Control animals were treated in a identical fashion with 5 μl of vehicle. For each compound, about 20 animals were used. All animal procedures were approved by the Institutional Animal Uses and Care Committee at the University of Oklahoma.

Six oxidation products (**1**, **2**, **3**, **4**, **5**, **6**, Scheme 2) of SAL in the presence of CySH were isolated and identified. Their structures were tentatively postulated based upon available UV, MS and NMR data.

2.3. Compound *1*

Compound **1** was isolated as a very light yellow solid. The UV spectrum of **1** in the HPLC mobile phase (6% MeCN, pH 3.0, TFA) exhibits bands at 260, 300 and 330 nm with an absorbance ratio of 1:0.25:0.13. FAB-MS (thioglycerol glycerol matrix) gave ion at $m/e = 515.0737$ (MH^+, 14.7%, $C_{19}H_{23}N_4O_7S_2$, calc. $m/e = 515.0729$). ^{1}H NMR (D_2O) δ 4.67 (t, ^{1}H, $J = 3.3$ Hz, C(b)–H), 3.97(t, 1H, $J = 5.55$ Hz, C(b″)–H), 3.87 (t, 1H, $J = 5.55$ Hz, C(b′)–H), 3.46–3.11 (m, 10H, C(a)–H_2, C(a′)–H_2, C(a″)–H_2, C(3)–H_2, C(4)–H_2). Homonuclear decoupling experiments revealed that the following resonance couples correlated to each other, 4.67 and 3.40, 4.67 and 3.16, 3.97 and 3.27, 3.87 and 3.40.

2.4. Compound *2*

Compound **2** was obtained as a very light yellow solid. The UV spectrum of **2** in the HPLC mobile phase (9% MeCN, pH3.0, TFA) exhibits bands at 256 and 328 nm with absorbance ratio of 1:0.14. FAB-MS (thioglycerol/glycerol matrix) gave ions at $m/e = 515.0694$ (MH^+, 20%, $C_{19}H_{23}N_4O_7S_3$, calc. $m/e = 515.0729$). ^{1}H NMR (D_2O) δ 4.57 (t, 1H, $J = 3.0$ Hz, C(b)–H), 3.93 (t, 1H, $J = 5.55$ Hz, C(b″)–H), 3.87 (t, 1H, $J = 5.85$ Hz, C(b′)–H), 3.54–3.1 (m, 10 H, C(a)–H_2, C(a′)–H_2, C(a″)–H_2, C(3)–H_2, C(4)–H_2). Homonuclear decoupling experiments revealed that the following resonance couples correlated to each other, 4.57 and 3.30, 3.93 and 3.24, 3.87 and 3.14.

MS and NMR data indicated that **1** and **2** are isomers. Their absolute configurations remain to be identified. The proposed structures of **1** and **2** are presented in this report.

2.5. Compound *3*

Compound **3** was isolated as a very light yellow powder. The UV spectrum of **3** in the HPLC mobile phase (50% MeCN, pH 3.0, TFA) exhibits bands at 220, 250 (sh), 280 (sh) and 314 nm with absorbance ratio of 1:0.8:0.37:0.17. FAB-MS (3-nitro-benzyl alcohol matrix) gave ion at $m/e = 835$ (MH^+, 1.4%, $C_{32}H_{46}O_{12}N_6S_4$). ^{1}H NMR (D_2O) δ 5.08 (q, 1H, $J = 6.9$ Hz, C(1′)–H), 4.66 (m, 1H, C(b)–H), 3.96 (t, 1H, $J = 5.4$ Hz, C(b′)–H), 3.87 (t, 1H, $J = 5.1$ Hz, C(b″)–H), 3.84 (t, 1H, $J = 5.7$ Hz, C(b‴)–H), 3.55–3.04 (m, 17 H, C(a)–H_2, C(a′)–H_2, C(a″)–H_2, C(a‴)–H_2, C(3)–H_2, C(3′)–H_2, C(4)–H_2, C(4′)–H_2, C(9)–H), 1.56 (d, 3H, $J = 6.9$ Hz, C(1)–CH_3), 1.52 (d, 3H, $J = 6.9$ Hz, C(1′)–CH_3). Homonuclear decoupling experiments revealed that the following resonance couples correlated to each other, 5.08 and 1.56, 4.66 and 3.40, 4.66 and 3.0, 3.96 and 3.30, 3.87 and

3.60, 3.84 and 3.2. The quartet at 4.8 ppm which belongs to C(1)–H was overlapped with the huge HDO peak. A COSY experiment revealed that the resonance at 1.52 (C(1)–CH_3) was correlated with the resonance at 4.8.

2.6. Compound **4**

Compound **4** was a very light yellow solid. The UV spectrum of **4** in the HPLC mobile phase (50% MeCN, pH 3.0, TFA) exhibits bands at 244, 282 (sh) and 318 nm with absorbance ration of 1:0.31:0.17. FAB-MS (3-nitro-benzyl alcohol matrix) gave ion at $m/e = 400.1005$ (MH^+, 100%, $C_{16}H_{22}N_3O_5S_2$, calc. $m/e = 400.1001$). ^1H NMR (D_2O) δ 4.99 (q, 1H, $J = 6.6$ Hz, C(1)–H), 4.55 (m, 1H, C(b)–H), 3.86 (t, 1H, $J = 6.0$ Hz, C(b′)–H), 3.53 (m, 2H, C(3)–H_2), 3.28 (m, 2H, C(a)–H_2), 3.15 (m, 3H, C(a′)–H_2, C(4)–H), 2.80 (m, 1H, C(4)–H, 1.55 (d, 3H, $J = 6.6$ Hz, C(1)–CH_3). Homonuclear decoupling experiments revealed that the following resonance couples correlated to each other, 4.99 and 1.55, 4.55 and 3.28, 3.86 and 3.15, 3.53 and 3.15, 3.53 and 2.80, 3.15 and 2.80.

2.7. Compound **5**

Compound **5** was isolated as a very light yellow solid. The UV spectrum of **5** in the HPLC mobile phase (38% MeCN, pH3.0, TFA) exhibits bands at 244, 280 and 322 nm with absorbance ratio of 1:0.35:0.16. FAB-MS (3-nitro-benzyl alcohol matrix) gave ion at $m/e = 400.1008$ (MH^+, 100%, $C_{16}H_{22}N_3O_5S_2$, calc. $m/e = 400.1001$). ^1H NMR (D_2O) δ 4.66 (q, 1H, $J = 6.9$ Hz, C(1)–H), 4.55 (m, 1H, C(b)–H), 3.77 (t, 1H, $J = 5.85$ Hz, C(b′)–H), 3.53 (m, 2H, C(3)–H_2), 3.31–3.20 (m, 4H, C(a)–H_2, C(4)–H_2), 3.13 (d, 2H, $J = 5.85$ Hz, C(a′)–H_2), 1.59 (d, 3H, $J = 6.9$ Hz, C(1)–CH_3). Homonuclear decoupling experiments revealed the following resonance couples correlated to each other, 4.66 and 1.59, 4.45 and 3.23, 3.77 and 3.13, 3.53 and 3.23.

2.8. Compound **6**

Compound **6** was isolated as very light yellow solid. The UV spectrum of **6** in the HPLC mobile phase (50% MeCN, pH 3.0, TFA) exhibits bands at 244, 280 and 310 nm with absorbance ratio of 1:0.32:0.155. FAB-MS (3-nitro-benzyl alcohol matrix) gave ion at $m/e = 400.1011$ (MH^+, 41.9%, $C_{16}H_{22}N_3O_5S_2$, calc. $m/e = 400.1001$). ^1H NMR (D_2O) δ 5.02 (q, 1H, $J = 6.6$ Hz, C(1)–H), 4.47 (t, 1H, $J = 3.6$ Hz, C(b)–H), 3.80 (t, 1H, $J = 5.55$ Hz, C(b′)–H), 3.54 (m, 2H, C(3)–H_2), 3.34–3.11 (m, 4H, C(a)–H_2, C(a′)–H_2), 2.93 (m, 1H, C(4)–H), 2.70 (m, 1H, C(4)–H), 1.55 (d, 3H, $J = 6.6$ Hz, C(1)–CH_3). Homonuclear decoupling experiments revealed that the following resonance couples correlated to each other, 5.02 and 1.55, 4.47 and 3.23, 3.80 and 3.18, 3.54 and 2.93, 3.54 and 2.70, 2.93 and 2.70.

3. Results

3.1. Cyclic voltammetric studies

Cyclic voltammograms of SAL (1 mM) dissolved in pH 7.4 phosphate buffer (μ 1.0) at a pyrolytic graphite electrode (PGE) using sweep rate of 10, 100 and 500 mV/s are presented in Fig. 1(a–c). SAL exhibits a dominant oxidation peak Ia and an unresolved pre-peak IIa which must be caused by the absorption of SAL on the electrode. After the scan reversal, the cathodic peak Ic which coupled with peak Ia reversibly can only be observed at a higher scan rate, indicating that the species formed upon oxidation (peak Ia) is fairly reactive at the condition employed. Concurrently, a cathodic adsorption peak IIc that is coupled with peak IIa has also been observed. Based upon our previous report [10,11], peak Ia results from the electrooxidation of SAL as a 2e, $2H^+$ reaction to give the *o*-quinone E (Scheme 1). Peak Ic corresponds to the reversible reduction of E back to SAL. The presence of cysteine caused significant changes in cyclic voltammograms of SAL. At a sweep rate of 10 mV/s, cyclic voltammograms of SAL exhibit, besides a rather ill-defined adsorption anodic pre-peak IIa, a domi-

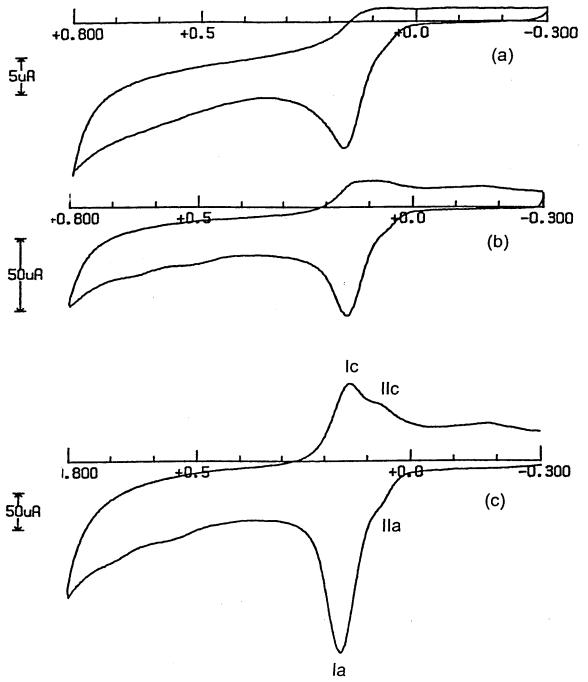

Fig. 1. Cyclic voltammograms at PGE of SAL (1 mM) in pH 7.4 phosphate buffer; (a) 10 mV/s, (b) 100 mV/s, (c) 500 mV/s.

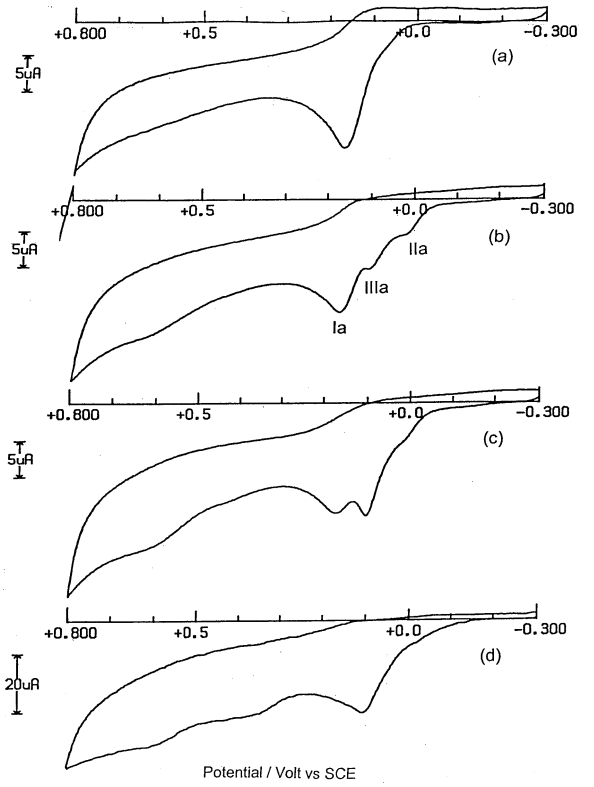

Fig. 2. Cyclic voltammograms at PGE of SAL in the presence of cysteine in pH 7.4 phosphate buffer. Scan rate 10 mV/s. (a) SAL (1 mM), (b) 1 mM SAL and 0.5 mM cysteine, (c) 1 mM SAL and 1 mM cysteine, (d) 1 mM SAL and 5 mM cysteine.

nant anodic peak Ia with the peak potential of 166 mV (Fig. 2(a)). By increasing the concentration of cysteine (0–5 mM), a new oxidation peak IIIa appeared (Ep = 90 mV) at a more negative potential than peak Ia. Correspondingly, the height of peak IIIa increased and ultimately became a dominant peak and merged with peak Ia at cysteine concentrations of higher than 5 mM. At the same concentration of cysteine (1 mM), an increase of the scan rate resulted in the positive shift of peak IIIa. As a consequence, peak IIIa and peak Ia merged at scan rate higher than 500 mV/s (Fig. 3). At a sweep rate of 500 mV/s, the CV of SAL shows a cathodic peak Ic which coupled reversibly with peak Ia. Increasing the concentration of cysteine led to the gradual disappearance of peak Ic which virtually disappeared when cysteine exceeded 5 mM (Fig. 4).

The above results indicated that a rapid reaction occurred between the *o*-quinone E and cysteine to produce the species responsible for the oxidation peak IIIa.

3.2. Controlled potential electrooxidation

Our previous study [10] has revealed that electrooxidation of SAL under physiological conditions gave *cis*-1,2,3,4-tetrahydro-1-methyl-4,6,7-isoquinoline triol (A), *trans*-1,2,3,4-tetrahydro-1-methyl-4,6,7-isoquinoline triol (B), 2,3,4-trihydro-1-methyl-7-hydroxy-6-oxyisoquinoline (C) and 1-methyl-6,7-isoquinoline diol (D) as major products. In this study, the oxidation of SAL was performed in the presence of cysteine. The controlled potential electrooxidation of SAL (1 mM) in the presence of cysteine (5 mM) in pH 7.4 phosphate buffer at 90 mV for 30 min produced in excess of 40 peaks (Fig. 5). Inspection of the chromatogram indicates that none of the major peaks belongs to A, B, C or D. The peak assigned to SAL is due to unreacted SAL. Using prepara-

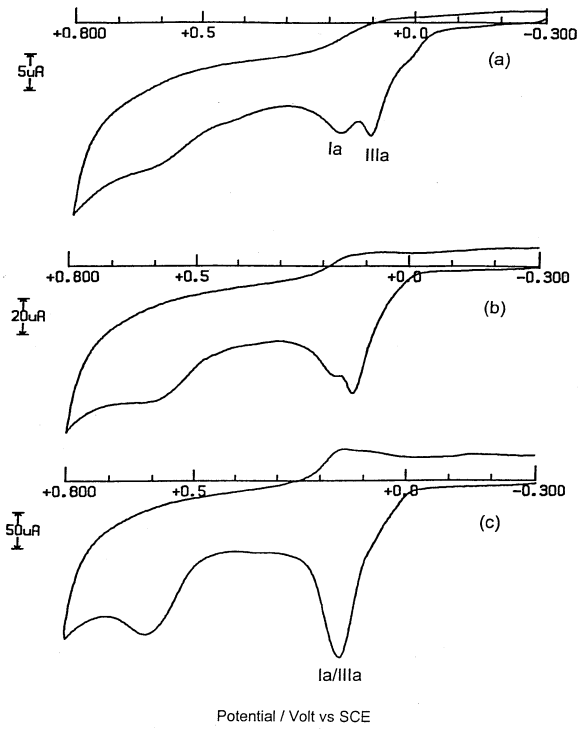

Fig. 3. Cyclic voltammograms at PGE of 1 mM SAL and 1 mM cysteine in pH 7.4 phosphate buffer at sweep rates of (a) 10 mV/s, (b) 100 mV/s and (c) 500 mV/s.

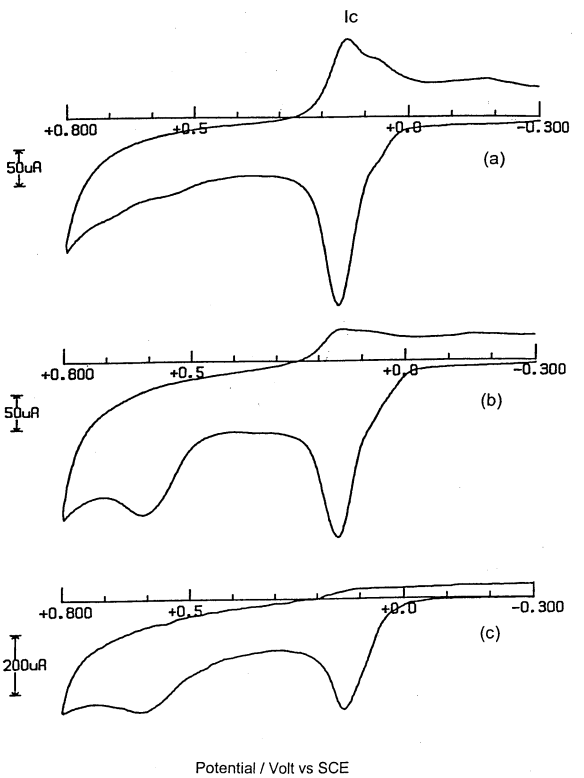

Fig. 4. Cyclic voltammograms at PGE of 1 mM SAL (a), 1 mM SAL and 1 mM cysteine (b), 1 mM SAL and 5 mM cysteine (c) in pH 7.4 phosphate buffer. Sweep rate 500 mV/s.

tive HPLC, six of the major products were isolated and structurally characterized, i.e. **1**, **2**, **3**, **4**, **5**, and **6**. Their structures are presented in Scheme 2.

In order to prepare sufficient quantities of products formed upon electrochemical oxidation of SAL in presence of cysteine, 17 mg of SAL·HCl and 48 mg of cysteine were dissolved in 80 ml of pH 7.4 phosphate buffer. Controlled potential electrooxidation of this solution was then carried out at 90 mV at PGE for 30 min. During the course of oxidation, the initially colorless solution turned to pale yellow. After termination of the reaction, 10–30 ml of the filtered solution was pumped into a Spherisorb reversed phase HPLC column and eluted using HPLC Method I. The effluent corresponding to compounds **1**, **2**, **3**, **4**, **5**, and **6** were individually collected and cooled with dry-ice. The solutions containing **1** and **2** were freeze-dried and then dissolved in a minimum volume of water and further purified by HPLC Method II. Compound **1** eluted at 13 min, **2** eluted at 17 min. The collected eluants containing **1** and **2** were freeze-dried. The solutions containing **3**, **4**, **5**, and **6** were further purified on a Regis preparative column using HPLC Method III. Compound **3** eluted at 27 min, **4** eluted at 28 min, **5** eluted at 23 min, **6** eluted at 30 min. After subsequent freeze drying, the purified solids of **3**, **4**, **5**, and **6**.were then identified.

3.3. Preliminary biological studies

Due to the complexity of the product mixture obtained upon oxidation of SAL in the presence of cysteine, the ability to isolate large quantities of products **1**, **2**, **3**, **4**, **5**, and **6** is limited. Accordingly, it has not yet been possible to perform extensive investigations into the biological activities of these compounds. However, as a initial screen for their in vivo activity, a 100 μg dose of each compound was dissolved in 5 μl of isotonic saline and injected

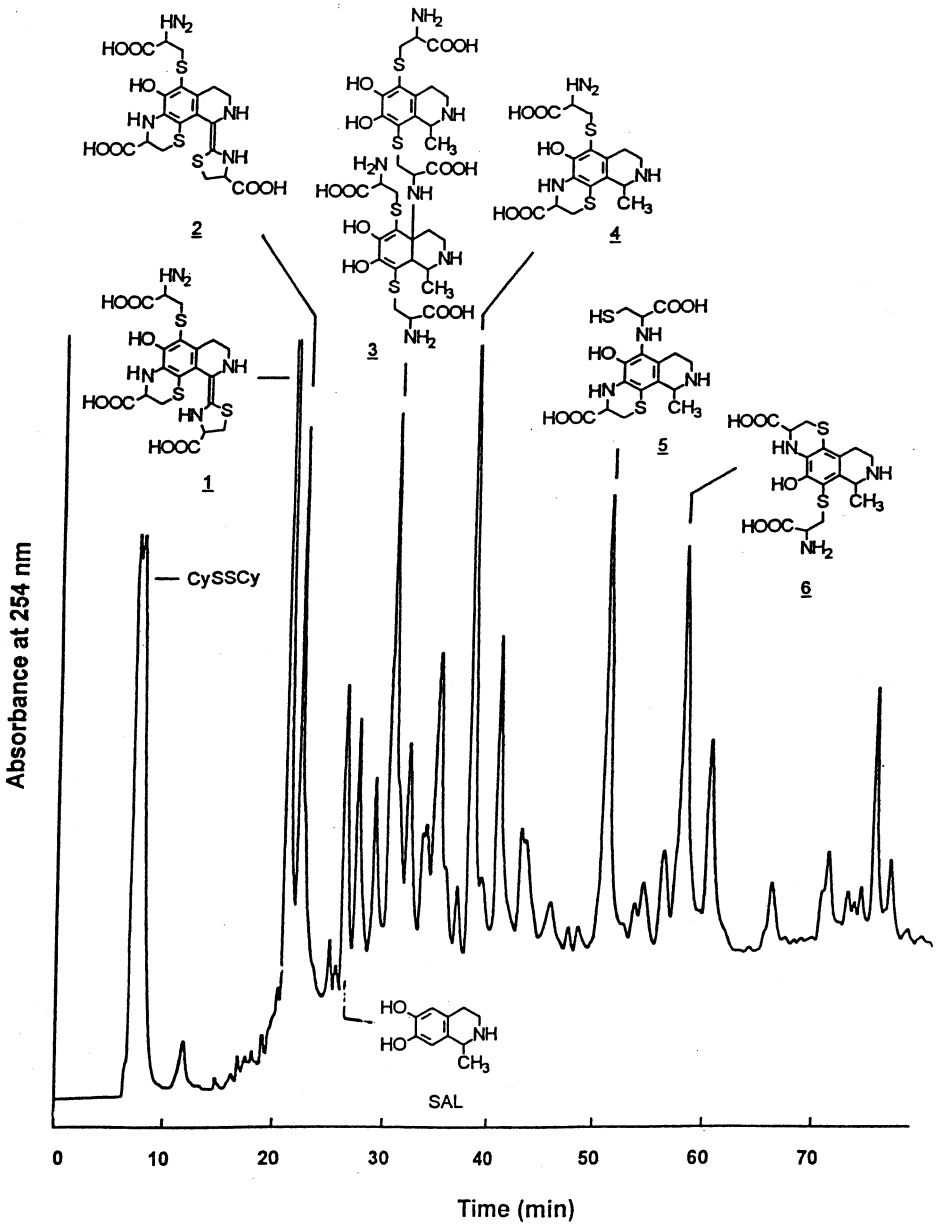

Fig. 5. HPLC chromatogram of the product solution obtained following controlled potential electrooxidation of 1 mM SAL and 5 mM cysteine at 90 mV for 30 min in pH 7.4 phosphate buffer. HPLC Method I with injection volume of 5 ml.

into the brain of laboratory mice in the vicinity of the right lateral ventricle. Compound **1** and compound **2** were not lethal at this doses and evoked no unusual behavioral responses. Compound **3** (100 μg) caused animals to tremor, jump, roll over, and stretch legs for 10–30 min, followed by a gradual recovery after 1 h. Behavior responses evoked by intracerebral injection of **4** at 25–100 μg doses include body tremor, jerking, difficulty to stand steadily, jumping around and rolling over with legs in running motion. Over 50 μg doses of **4** caused all of the animals die within

30 min. Animals treated with **5** (50–100 μg) were generally unable to stand up, their bodies arched backward, they jumped around, rolled over and also exhibited tremoring and stiff tail. At times, the animals scratched their head or mouth with the front limbs vigorously. Compound **5** (100 μg), caused death of all experimental animals within 30 min. Compound **6** (12.5–100 μg doses) evoked episodes of repetitive, violent rolling along the head–tail axis and violent jumping, generally, had difficulty to stand still and repetitively stepped backward with apparent loss of hindlimb function. More than 25 μg of **6** caused all the animals to die.

3.4. Reaction pathway

In the physiological pH domain, electrochemical oxidation of SAL generates four major products A, B, C and D [10] (Scheme 1) via the proximate SAL *o*-quinone E as the intermediate. Since E is very unstable at neutral pH but appreciably more stable in acidic medium, E was prepared in 0.1 M HCl by electrooxidation [11]. It was also demonstrated that E could readily react with cysteine to produce 8-*S*-cysteinylsalsolinol (F) which can be easily oxidized to G followed by cyclization and reduction to yield the benzothiazine I at physiological pH as depicted in Scheme 1 [11]. In this report, the oxidation chemistry of SAL was investigated in the presence of cysteine at neutral pH. Cyclic voltammograms of SAL in the presence of cysteine at pH 7.4 (Figs. 2–4) support the conclusion that the *o*-quinone E generated from the oxidation of SAL reacts with this sulfhydryl compound that diverse the formation of A, B, C and D. This conclusion was support by the fact that controlled potential oxidation of SAL in the presence of cysteine excluded the formation of A, B, C, and D (Fig. 5). For comparison purposes, 8-*S*-cysteinylsalsolinol was synthesized as we reported [11] and its cyclic voltammogram at PGE in pH 7.4 phosphate buffer is presented in Fig. 6(b). Also presented are the cyclic voltammograms of SAL in presence of cysteine and the cyclic voltammograms of **1**, **2**, **3**, **4**, **5**, and **6**. The peak potential Ep for peak IIIa in the cyclic voltammogram of SAL observed in the presence of cysteine

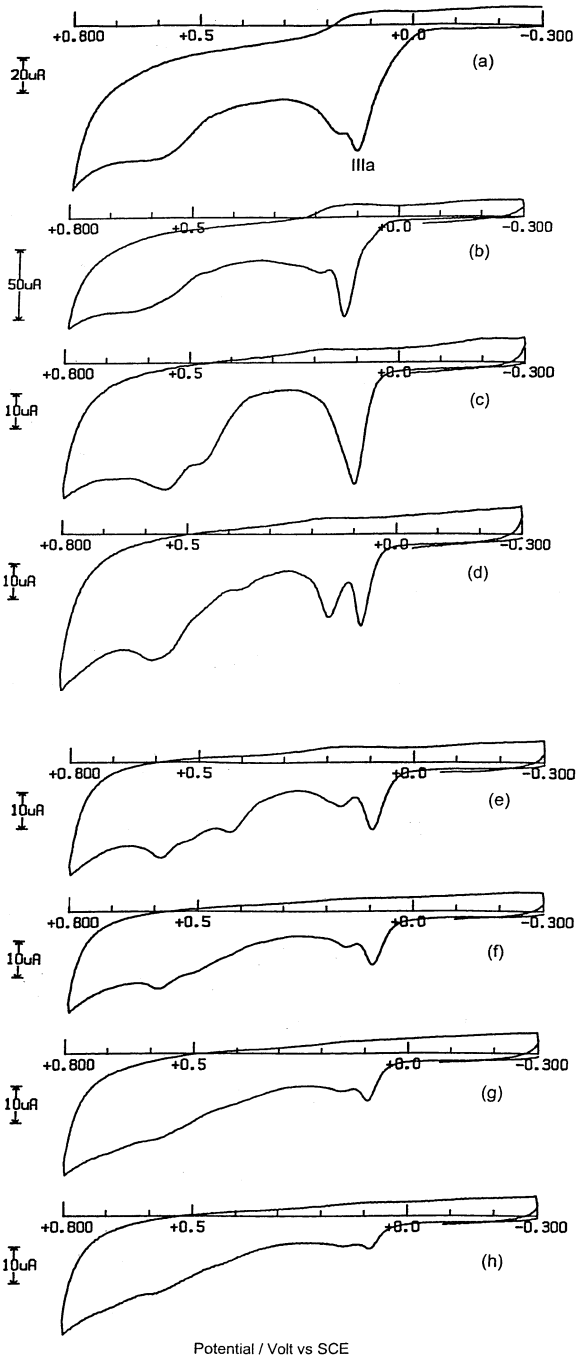

Fig. 6. Cyclic voltammograms at PGE. pH 7.4 phosphate buffer. Sweep rate 100 mV/s. (a) SAL (1 mM) and 1 mM cysteine, (b) 1 mM 8-*S*-cysteinylsalsolinol, (c) **1**, (d) **2**, (e) **3**, (f) **4**, (g) **5**, (h) **6**.

(Fig. 6(a)) is quite close to the oxidation peak potential of 8-*S*-cysteinylsalsolinol (Fig. 6(b)). Hence it is very probable that peak IIIa corresponds to the oxidation of 8-*S*-cysteinylsalsolinol (F) which is formed as a result of the nucleophilic addition of cysteine to the *o*-quinone E, the proximate oxidation product of SAL. In order to account for the various products formed from oxidation of SAL in the presence of cysteine, a mechanism is proposed in Scheme 2. It appears probable that F is oxidized to the corresponding *o*-quoinone G. The fact that the oxidation peak potential of F is lower than that of SAL indicated that F is very easily oxidizable. The 8-*S*-cysteinylsalsolinol-*o*-quinone G might be attacked by another molecule of cysteine to give 2,8-*S*-bicysteinylsalsolinol J or it could be cyclized to form the *o*-quinone imine H. The electrophilic *o*-quinone H can also react with the sulfhydryl or amino residues of cysteine to yield **4** and **5** which have been isolated and structurally identified. The cyclic voltammogram of **4** (Fig. 6(f)) indicated that **4** is also a rather easily oxidizable species, and might be further oxidized to the corresponding *o*-quinone imine K. Subsequent tautomerization and oxidation of K could produce quinone methide compound L. Nucleophilic attack of L by cysteine can generate M, followed by the reaction sequence of cyclization, oxidation and tautormerization, as shown in Scheme 2, to produce the final products **1** and **2** which have been isolated and structurally identified. By analogy, the 2,8-*S*-bi-cysteinylsalsolinol J must also be an easily oxidizable species to generate the corresponding *o*-quinone N. Cyclization and reduction of N could yield **6**. Nucleophilic addition of the amino moiety of J to the species N along with reduction by cysteine may result in the formation of **3**. Fig. 6(c–h) indicates that the isolated products **1**, **2**, **3**, **4**, **5**, and **6**, are more easily oxidizable than SAL. Our experiments also demonstrated that they can only be isolated at the early electrooxidation stage of SAL in the presence of cysteine. Prolonged oxidation leads to the disappearance of these products and gives an even more complicated mixture which remains to be investigated.

4. Conclusions

Collin [14] advanced a hypothesis that oxidation of SAL and other TIQs which are elevated in the brain of intoxicated alcoholics might lead to the formation of toxic metabolites that are responsible for the neurodamage. We [15] recently demonstrated that the oxidation product C (Scheme 1) derived from SAL is indeed a behavioral toxin when administrated into the brain of laboratory animals. The results presented in this report indicate that if oxidation of SAL occurs in presence of cysteine, such as inside in the brain, the oxidation pathway of SAL diverges significantly and the chemistry would be extremely complex with the formation of many products. (Fig. 5). 8-*S*-cysteinylsalsolinol (F) and dihydrobenzothiazine (I) (Scheme 1) would be expected to be formed. However, the fact that they are not among the major products founded must be due to their further oxidation. The isolated benzothiazine species **1**, **2**, **3**, **4**, **5**, and **6** are more easily oxidizable than SAL and as a result the oxidation of SAL must be elevated. Furthermore, in vivo experiments revealed that, **3**, **4**, **5**, and **6** are lethal when centrally administered into the mouse brain and evoked profound behavioral responses. These observations propose the hypothesis that whenever the oxidation of SAL occurs intraneuronally, the reaction sequences shown in Scheme 2 may happen to give one or more of the products indicated. They are toxins and/or neuropharmacologically active agents which may play a role in the neurodegenerative, behavioral and addictive consequences of ethanol consumption.

References

[1] H.S. Raper, Physiol. Rev. 8 (1928) 245–282.
[2] R. Crippa, V. Horak, G. Prota, P. Svornos, L. Wolfrom, The Alkaloids, vol. 36, 1989, pp. 253–323.
[3] S. Ito, E. Novellino, F. Chioccara, G. Misuraca, G. Prota, Experimentia 36 (1980) 822–823.
[4] A. Palumbo, G. Nardi, M. d'Ischia, G. Misuraca, G. Prota, Gen. Pharmacol. 14 (1983) 253–257.
[5] J.P. Benedetto, J.P. Ortonne, C. Voulot, C. Khatchadourian, G. Prota, J. Thirolet, J. Invest. Dermatol. 79 (1982) 422–424.

[6] M.A. Collins, in: H. Begleitier (Ed.), Advances in Experimental Medicine and Biology, vol. 126, Plenum Press, New York, 1982, pp. 87–102.
[7] K. Matsubara, S. Fukishma, Y. Fukui, Brain Res. 413 (1987) 336–343.
[8] M.A. Collins, W.P. Num, G. Borge, G. Teas, C. Goldfarb, Science 206 (1979) 1184–1186.
[9] G. Cohen, M.A. Collins, Science 167 (1970) 1749–1751.
[10] F. Zhang, G. Dryhurst, Bioorg. Chem. 19 (1991) 384–397.
[11] F. Zhang, G. Dryhurst, Bioorg. Chem. 21 (1993) 221–237.
[12] G. Christian, W.C. Purdy, J. Electroanal. Chem. Interf. Electrochem. 3 (1962) 363–367.
[13] J.L. Owens, H.A. Marsh, G. Dryhurst, J. Electroanal. Chem. Interf. Electrochem. 91 (1978) 231–247.
[14] M.A. Collin, Trends Pharmacol. Sci. 3 (1982) 373–375.
[15] F. Zhang, G. Dryhust, J. Med. Chem. 36 (1993) 11–19.